IOP Concise Physics

Electronic Structure of Organic Semiconductors

Polymers and small molecules

Luís Alcácer

Chapter 6

Computational methods

There are many computational methods for the calculation of energy levels and orbitals in molecules, as well as for energy bands in solids. Here, we will mention briefly the general principles which support computational methods based on the Hartree–Fock (HF) approximation and on density functional theory (DFT). We will consider the electronic structures of molecules first, and then that of solids.

6.1 Hartree–Fock theory

In the HF approximation, the interactions of each electron with all the other $N - 1$ are reduced to a mean field potential, $V(\mathbf{r})$, which depends only on its own coordinates, $\mathbf{r}$ (figure 6.1).

The HF method is based on the one-electron equation

$$f\ \chi_a = \varepsilon_a\ \chi_a \tag{6.1}$$

where f is the Fock operator. χ_a are the spin-orbital functions which are the product of the spatial wave functions $\psi_a(\mathbf{r})$ with the spin functions $\sigma_a(\omega)$, where ω are the spin coordinates:

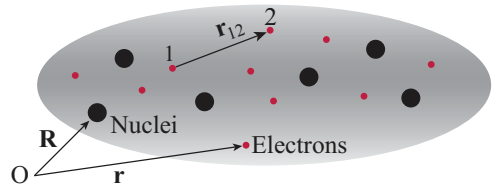

Figure 6.1. In the Hartree–Fock approximation, the interactions of each electron with the other $N - 1$ are reduced to a mean field potential, $V(\mathbf{r})$, which depends only on its own coordinates, $\mathbf{r}$. $\mathbf{R}$ are the coordinates of the nuclei. Electrons 1 and 2 interchange the space+spin coordinates.

doi:10.1088/2053-2571/aaddd8ch6

$$\chi_a(\mathbf{x}) = \psi_a(\mathbf{r})\sigma_a(\omega). \tag{6.2}$$

For the general case of a system of N electrons and M nuclei, and noting that the sum extends to all *occupied spin-orbitals* (occso), we have for the Fock operator

$$f = h + \sum_{b=1}^{\text{occso}} (J_b - K_b) \tag{6.3}$$

with[1] $h = -\frac{1}{2}\nabla^2 + \sum_A^M \frac{Z_A}{|\mathbf{r} - \mathbf{R}_A|}$, in which the first and second terms are the kinetic energy and the attractive electron–nuclei potential, respectively. J and K are the Coulomb and exchange integrals:

$$J_b = \int |\psi_b(\mathbf{r}_2)|^2 \frac{1}{r_{12}} d\tau_2 \tag{6.4}$$

$$K_b = \int \psi_b^*(\mathbf{r}_2)\psi_a(\mathbf{r}_2)\frac{1}{r_{12}} d\tau_2. \tag{6.5}$$

Note that in these integrals, and since we consider the interactions of each electron with each one of the others, it is common to designate electron 1, of coordinates $\mathbf{r}_1$, the electron which is in the reference position, and electron 2, of coordinates $\mathbf{r}_2$, the other one, whose interaction electron 1 is feeling. For a system of N electrons, we can write $V_{ee}(1) \equiv V_{ee}(\mathbf{r}_1) \equiv V_{ee}(\mathbf{r})$ (see figure 6.1).

Note also that in equation (6.3) the sum goes from $b = 1$ and extends to all *occupied spin-orbitals* (occso), including $b = a$ (the reference orbital, where electron 1 is). Introducing $b = a$, which means to account for the *self-interaction*, does not bring any problems, since, if we make $b = a$ in equations (6.4) and (6.5), we get $J = K$, which cancel in V_{ee}.

The Hamiltonian for a system of N electrons and M nuclei can be written as a sum of Fock operators:

$$H = \sum_{i=1}^{N} f(i) \tag{6.6}$$

where the *spin-orbitals* $\chi_a(\mathbf{x})$, are the solutions of the HF equations, of the form

$$f\ \chi_a = \varepsilon_a\ \chi_a. \tag{6.7}$$

The problem is now reduced to building the f operator (6.3), for which we need the χ_a which are the solutions of the HF equations. To do that, we need to follow an iteration procedure, starting with a set of chosen *spin-orbitals* $\{\chi_a\}$.

From the known $\{\chi_a\}$ spin-orbitals, we can write an expression for the energy, considering that:

[1] In quantum chemical calculations, it is convenient to use *atomic units* (see appendix A).

- the one-electron integrals contribute with a term h_{aa} for each electron in spin orbital a;
- the two-electron integrals contribute a term J_{ab} for each pair of electrons, and a term $-K_{ab}$ for each pair of electrons with parallel spins.

We could now proceed to distinguish between *closed shell* systems and *open shell* systems to get the restricted HF (RHF) and the unrestricted HF (URHF) versions.

In any case, to solve the HF equations of the form

$$f\psi_a = \varepsilon_a \psi_a \tag{6.8}$$

where ψ_a is the spatial part of χ_a, we need a basis of functions (e.g. Slater type orbitals, STO, and Gaussian type orbitals, GTO) to build linear combinations (Roothaan's method [1]). The iterative calculation proceeds with the diagonalization of the Fock matrix **F**, of all matrix elements of the Fock operator.

In figure 6.2, we show diagrams of the energy levels in the UHF and in the RHF versions.

The ε_a values of equation (6.8) have a physical meaning. According to Koopmans' theorem, the ionization potential is equal to the negative of the energy of the spin-orbital χ_n from which one electron is removed, i.e.

$$IP = E_{N-1} - E_N = -\varepsilon_n. \tag{6.9}$$

On the other hand, the electron affinity is the energy released when one electron is added to a given spin-orbital χ_m.

$$EA = E_N - E_{N+1} = -\varepsilon_m. \tag{6.10}$$

In the above equations, it is assumed that χ_n was occupied and that χ_m was empty for the system with N electrons. Therefore, the first ionization potential is $IP_{\text{first}} = -\varepsilon_{\text{HOMO}}$ (figure 6.3).

In quantum chemistry, the electronic structure of atoms and molecules can be described in terms of orbitals and energy levels calculated for one electron, which

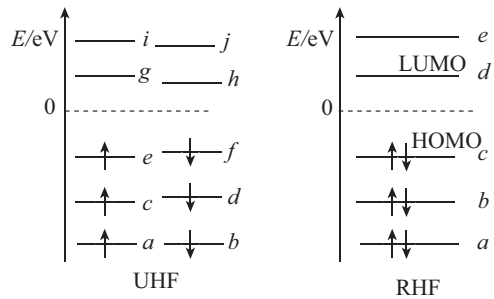

Figure 6.2. Diagrams of the molecular energy levels in the unrestricted Hartree–Fock (UHF) and in the restricted Hartree–Fock (RHF) versions. The RHF can be used for *closed shell* systems and the UHF has to be used for systems with incomplete shells. Note the highest occupied molecular orbital (HOMO) and the lowest unoccupied molecular orbital (LUMO).

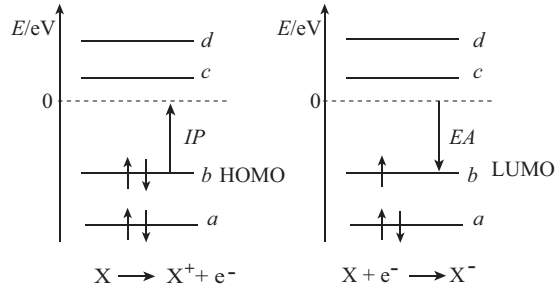

Figure 6.3. Ionization potential (IP) and electron affinity (EA) for the removal of an electron from spin-orbital χ_b and the addition of an electron to spin-orbital χ_b, respectively.

moves in the field of the nuclei and in the mean field of the interactions with all other electrons. The distribution of the electrons by the spatial orbitals is the *electronic configuration*. The electronic states resulting from these configurations are the *terms of the configurations*. The many-electron states can only be described in terms of eigenfunctions of total angular momentum, since the individual angular momentum of each electron is not an *observable*—the interactions of various types, namely the Coulomb, spin and exchange, do not allow that the many-electron wave function be simple products of the one-electron wave functions. It is therefore pertinent to distinguish between *levels* (and *orbitals*), *electronic configurations* and *electronic states*, which are illustrated in figure 6.4. It is also important to consider the notation: lower case for levels (and orbitals) and upper case for many-electron states, for atoms. For molecules, the corresponding notation is in Greek letters.

Equation (6.6) may suggest that the wave function for the N electron system could be a product of all occupied χ_a. But all electrons are *identical* and can exchange (consider the K integrals)—one electron can simultaneously occupy all orbitals—and are correlated—*entangled* in Schrödinger's words[2], meaning that the knowledge about one of them is *inextricably* linked to the knowledge about the others—and therefore the wave function has to be written as an anti-symmetrized product of all permutations, or a Slater determinant:

$$\Psi = \frac{1}{\sqrt{N!}} \begin{vmatrix} \chi_a(\mathbf{x}_1) & \chi_b(\mathbf{x}_1) & \cdots & \chi_n(\mathbf{x}_1) \\ \chi_a(\mathbf{x}_2) & \chi_b(\mathbf{x}_2) & \cdots & \chi_n(\mathbf{x}_2) \\ \cdots & \cdots & \cdots & \cdots \\ \chi_a(\mathbf{x}_N) & \chi_b(\mathbf{x}_N) & \cdots & \chi_n(\mathbf{x}_N) \end{vmatrix} \tag{6.11}$$

where the $\mathbf{x}_i$ are the space+spin coordinates of the electrons.

[2] The word 'entangled' was coined in Schrödinger's article about his famous cat, E Schrödinger 1935 The Present Situation in Quantum Mechanics *Naturwiss.* **23** 807 translated into English in 'Quantum Theory and Measurement' 1983 eds J A Wheeler and W H Zurek (Princeton, NJ: Princeton University Press). A video about Schrödinger's cat can be seen at http://www.youtube.com/watch?v=CrxqTtiWxs4.

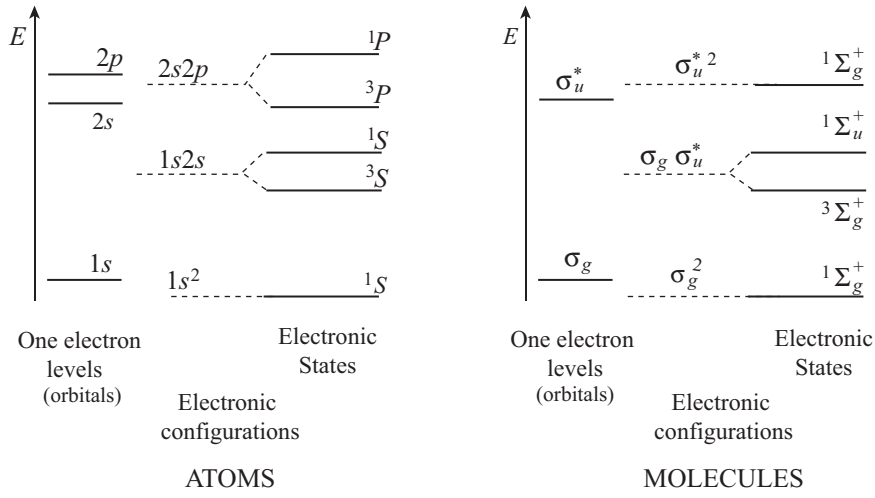

Figure 6.4. Illustration of the differences between orbital energy levels, electronic configurations and electronic states.

In the HF method, the Fock operator is of the form $f = h + \sum_b^{\text{occso}}(J_b - K_b)$ in the basis of the spin-orbitals χ, with $h = -\frac{1}{2}\nabla^2 - \sum_A \frac{Z_A}{|\mathbf{r} - \mathbf{R}_A|}$, implying that the total electronic energy will be given by

$$E_{\text{HF}} = \sum_a^{\text{occso}} h_{aa} + \frac{1}{2}\sum_a^{\text{occso}}(J_{ab} - K_{ab}). \tag{6.12}$$

In the Φ basis of the linear combinations, we can write the matrix equation $\mathbf{X} = \Phi\mathbf{C}$ with components $\chi(\mathbf{x}) = \psi(\mathbf{r})\sigma(\omega)$ and taking the *density matrix* as $\mathbf{D} = \mathbf{C}\mathbf{C}^{\dagger}$, we will have, considering that for any T operator, $\langle T\rangle = \text{tr}(\mathbf{DT})$:

$$E_{\text{HF}} = \text{tr}(\mathbf{DH}) + \frac{1}{2}\text{tr}(\mathbf{DJ}) - \frac{1}{2}\text{tr}(\mathbf{DK}). \tag{6.13}$$

6.2 Density functional theory (DFT)

Presently, one of the most successful methods for the calculation of the electronic structure of molecules and solids is that of DFT. The theory is based on the assumption that the total energy of a system, including all interactions (exchange and correlation), is a unique functional of the *electron density*, and that the minimum of this functional is the energy of the *ground state* [2]. The appeal of this method lies in the fact that, in principle, the wave function for a system of N electrons, which is a function of 4N coordinates (3N space coordinates and N spin coordinates) can be replaced by the electron density, which is a function of only three space coordinates.

The problem of the N electrons can then be solved, by solving the system of self-consistent monoelectronic equations—the Kohn–Sham equations [3]. These equations which are identical to the HF equations can be solved by similar iterative methods. The Kohn–Sham equations are of the form

$$f^{KS}\,\chi_a = \varepsilon_a\,\chi_a \tag{6.14}$$

where f^{KS} is the Kohn–Sham operator; χ_a, the Kohn–Sham *spin-orbitals*, and ε_a is the energy of spin orbital a.

The Kohn–Sham operator

$$f^{KS} \;=\; T + V_{KS}(\mathbf{r}) \tag{6.15}$$

is the sum of the kinetic energy $T = -\frac{1}{2}\nabla^2$ and an effective potential called the Kohn–Sham potential, V_{KS}, which is a functional of the electron density, $\rho(\mathbf{r})$, and is of the form

$$V_{KS}[\rho(\mathbf{r})] = V_{\text{ext}}(\mathbf{r}) + V_{\text{Hartree}}[\rho(\mathbf{r})] + V_{XC}[\rho(\mathbf{r})]. \tag{6.16}$$

$V_{\text{ext}}(\mathbf{r})$ is an external potential, generally the attractive potential between the electrons and the nuclei, V_{ne}.

$$V_{\text{ext}}(\mathbf{r}) = V_{ne}(\mathbf{r}) = -\sum_A \frac{Z_A}{|\mathbf{r} - \mathbf{R}_A|}. \tag{6.17}$$

V_{Hartree} is the term relative to the Hartree approximation, i.e. the mean field felt by one electron, due to the Coulomb interactions with all others,

$$V_{\text{Hartree}} = \int d\tau' \frac{\rho(\mathbf{r}')}{|\mathbf{r} - \mathbf{r}'|}. \tag{6.18}$$

It is identical to the Coulomb integral J of HF theory, but now a functional of ρ, i.e. $V_{\text{Hartree}} = J[\rho]$. Finally, V_{XC} is the *exchange-correlation* term, or XC, and contains all *exchange*, V_X, and *correlation*, V_C, contributions; ($V_{XC} = V_X + V_C$).

It is defined as

$$V_{XC} = \frac{\delta E_{XC}}{\delta \rho} \tag{6.19}$$

and is, naturally, the more problematic term. There are many choices available for approximate functionals. One of the simplest is the *local density functional* (LDF) or *local density approximation* (LDA) for which the exchange-correlation, E_{XC}, is the energy of a homogeneous electron gas of constant density ρ, of which there are databases from Monte Carlo calculations. We will not go into more detail concerning the various V_{XC} potentials in this concise text.

The *electron density* is defined in terms of the *Kohn–Sham spin-orbitals*:

$$\rho_0(\mathbf{r}) = \rho_{KS}(\mathbf{r}) = \sum_{a}^{\text{occso}} |\chi_a(\mathbf{r})|^2 . \tag{6.20}$$

Note that the sum extends over all *occupied spin-orbitals* (occso).

Expression (6.14) represents a set of coupled non-linear equations (one for each a) that depend on the *electron density* which appears in this theory as a *fundamental variable*.

For the purpose of computational calculations, a procedure can be used, which starts with an appropriately chosen *density* $\rho_0(\mathbf{r})$ to obtain a first V_{KS}. This potential is then introduced in the Kohn–Sham equations, which, when solved, give the Kohn–Sham orbitals and the energies. From these orbitals, a new density $\rho_0(\mathbf{r})$ is calculated and a new V_{KS}, and so forth until convergency. The self-consistent cycle is terminated when the pre-established criteria is met. The two most common criteria are based on the differences between the values of the total energies or on the values of the densities for two successive iterations. In other words, when $|E^{(i)} - E^{(i-1)}| < \delta_E$ or $\int |\rho^{(i)} - \rho^{(i-1)}| d\tau < \delta_\rho$ in which $E^{(i)}$ and $\rho^{(i)}$ are the values of the total energy or of the density for iteration i, and δ_E and δ_ρ are the tolerances defined by the user.

When a basis for the *Kohn–Sham orbitals* is used (Gaussian or Slater type), it is necessary to diagonalize the matrix $\mathbf{F}^{\text{KS}}$ as in the Hartree–Fock–Roothaan method. It should be noted that the minimization of the energy is made using the Lagrange multipliers, in which the restrictive condition, equivalent to normalization is in DFT, $\int \rho(\mathbf{r}) d\tau = N$.

In the end, one can calculate the various observables, such as the total energy. From that, one can obtain equilibrium configurations by minimization of $E(\mathbf{R})$, ionization energies, etc. In the Kohn–Sham theory, the total energy is given by expressions which are similar to those of HF theory, but taking into account the Kohn–Sham operator and the fact that the fundamental variable is the *electron density*.

In DFT, we will have, identically to equation (6.13):

$$E_{\text{DFT}} = \text{tr}(\mathbf{DH}) + \frac{1}{2}\text{tr}(\mathbf{DJ}) + E_X[\mathbf{D}] + E_C[\mathbf{D}] \tag{6.21}$$

in which the terms $E_X[\mathbf{D}]$ and $E_C[\mathbf{D}]$ are the exchange and correlation terms, respectively, the last being neglected in HF theory. The HF theory is therefore a particular case of DFT, in which $E_X[\mathbf{D}] = -\frac{1}{2}\text{tr}(\mathbf{DK})$ and $E_C[\mathbf{D}] = 0$.

What is the meaning of the Kohn–Sham *spin-orbitals*? In principle, they do not have a physical meaning. They are used as a tool for the calculation of the *electron density* which is the fundamental variable of the theory. Its unique link to reality is that the sum of all their squares is equal to the real electron density [4]. Note that the molecular orbitals of HF theory are still worse—they do not take into account the correlation effects, nor do they give the real density.

One should also not mistake Slater determinants built from Kohn–Sham spin-orbitals, with the true wave function for the system of N electrons. In DFT, there is no exact wave function for the system. Also, the energies ε_a have no real meaning, since there is no equivalent to Koopmanns' theorem to relate the orbital energies to the ionization potentials, except that the $\varepsilon_{\max}$ (the HOMO-KS energy) is equal to the negative of the first ionization potential [5]:

$$\varepsilon_{\text{HOMO-KS}} = -IP. \tag{6.22}$$

The HOMO and LUMO levels can be approximately determined experimentally by several methods, both in solution or in a solid film, as discussed below (see section 6.2.1).

Although these computational methods are of great value to predict the properties of molecules and solids and help on the design of new materials, they may not give accurate energy values for the HOMO and LUMO orbitals and their relation to the ionization potential and electron affinity. In DFT calculations, the difficulty lies in finding the appropriate functional. The exact functional should give a HOMO energy exactly equal to minus the vertical ionization potential. On the other hand, the electron affinity should be minus the energy of the HOMO of the $N + 1$ electron system.

The prediction of the electron affinity, in particular, is unreliable as a consequence of the large effect of orbital relaxation on the LUMO energy value. Zhang *et al* [6] analyzed these difficulties and proposed ways to correct the values, based on experimental data of ionization potentials and lowest excitation energies. In particular, the following formula was proposed for several functionals

$$-E_{\text{HOMO}_{\text{corr}}} = A + B(-E_{\text{HOMO}_{\text{cal}}}) \tag{6.23}$$

where $E_{\text{HOMO}_{\text{corr}}}$ and $E_{\text{HOMO}_{\text{cal}}}$ are the corrected and the calculated HOMO energies, respectively. This empirical correction is a simple linear correlation but it gives improved values of the ionization potentials from the HOMO energies. For the B3LYP functional, for example, the authors found that a good correlation, ($R = 0.94$), is given for $A = -1.02$, $B = 0.93$. They conclude that all (11) functionals tested give accurate predictions for the HOMO energies when empirically corrected, and accurate HOMO–LUMO gaps by using time-dependent DFT methods or the differences between the corrected HOMO and LUMO energies. LUMO energies can best be obtained by adding the corrected HOMO energies to the HOMO–LUMO gaps.

6.2.1 Ionization potential, electron affinity and energy gaps

The energies of the HOMO and LUMO are of the greatest importance since they determine the electronic and optical properties of materials. There is, however, some confusion in the literature about the meaning and accuracy of these parameters in organic semiconductors. A clarification of that meaning, as well as that of the various types of energy gaps that can be measured or calculated by computational methods, is the focus of a succinct article by Jean-Luc Brédas [7]. The subject is also discussed in detail in Köhler and Bässler's book [8], and useful information on

experimental methods and corrections is given by Sworakowski [9]. Here, we will describe some of the most relevant of these authors' views and add a few words on the definition and meaning of some related concepts in metals and semiconductors.

As mentioned above, in the HF computational methods, according to Koopmans' theorem, the first ionization potential, *IP*, is considered to be minus the energy of the HOMO level ($IP = -\varepsilon_{\mathrm{HOMO}}$), and the first electron affinity, *EA*, minus the energy of the LUMO level ($EA = -\varepsilon_{\mathrm{LUMO}}$), i.e. 'the negative of the energy change when adding an electron to the neutral species', according to the IUPAC definition. In DFT, it is assumed that the $\varepsilon_{\max}$ (HOMO-KS energy) is equal to minus the first ionization potential.

In a molecule, the *optical gap*, ΔE_o, is considered as the energy of the lowest electronic transition. The difference between the first ionization potential and the first electron affinity is called the *fundamental gap* (also *chemical hardness*) ($\Delta E_f = IP - EA$) and it is only approximately given by the difference between the calculated HOMO and LUMO energy levels, which is the *HOMO–LUMO gap*. The optical gap is lower than the fundamental gap, due to the fact that in the first excited state, the electron–hole pair generated by the optical transition has a binding energy $E_b = \Delta E_f - \Delta E_o$ (see figure 6.5).

We should remind ourselves that the HOMO and LUMO correspond to one electron levels and not to many electron states (see figure 6.4), and that the energies calculated for those one electron levels differ from the experimentally needed energies to remove one electron from a neutral many electron molecule (the *IP*) or to add one electron to a neutral molecule (the *EA*). Therefore, the common practice to use the HOMO and LUMO energies as approximations to the *IP* and *EA* is misleading.

For a semiconductor, the electron affinity is the change in energy when one electron is moved from the vacuum to the bottom of the conduction band, $EA \equiv E_{\mathrm{vac}} - E_{\mathrm{c}}$. The band gap is the difference between the bottom of the conduction band, E_c, and the top of the valence band, E_v, and is considered to be

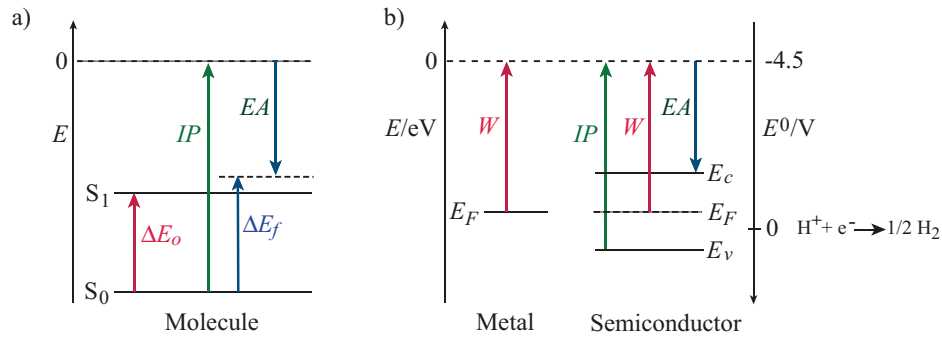

Figure 6.5. (a) Ionization potential (*IP*), electron affinity (*EA*), and gap energies (optical gap (ΔE_o) and fundamental gap (ΔE_f)) in molecules. (b) Work function (W), *IP* and *EA* in metals and semiconductors. E_c is the bottom of the conduction band, E_F is the Fermi energy and E_v is the top of the valence band. On the right, the electrochemical scale of reduction potentials (in volts) relative to the standard hydrogen electrode.

the difference between the ionization potential and the electron affinity. We should also define a *transport gap*, E_g, as the minimum energy needed to create a charge carrier. Figure 6.5(b) also shows the work function of a metal and a semiconductor as well as the ionization potential and electron affinity. The electrochemical scale of standard reduction potentials, E^0, in volts, is shown on the right, for comparison with the energy scale, in electron-volts.

Sworakowski [9] compiled a significant amount of data from the literature on small molecule organic semiconductors and showed that the electrochemical cyclic voltammetry measurements for the HOMO and LUMO energies are typically lower than the values obtained directly from UV photoelectron spectroscopy, UPS, and inverse photoelectron spectroscopy, IPES, measurements by *ca.* 16%. He proposed the following empirical equations for the first ionization potential and electron affinity based on the oxidation, E_{ox}, and reduction potentials, E_{red}, measured in solution or in contact with non-aqueous solvents of high dielectric constant,

$$IP = -E_{\mathrm{HOMO}} = \alpha^{+} \times (eE_{ox}) + \beta^{+} \tag{6.24}$$

$$EA = -E_{\mathrm{LUMO}} = \alpha^{-} \times (eE_{red}) + \beta^{-} \tag{6.25}$$

with $\alpha^{+} = (1.15 \pm 0.09)$, $\beta^{+} = (4.79 \pm 0.07)$ eV and $\alpha^{-} = (1.18 \pm 0.05)$, $\beta^{-} = (4.83 \pm 0.05)$ eV when measured against the Fc^{+}/Fc (ferrocenium/ferrocene) reference electrode at 25 °C. For polymers, he proposed $\alpha^{+} = (1.7 \pm 0.2)$ and $\beta^{+} = (4.6 \pm 0.1)$ eV.

To conclude, we enumerate below the most used methods to determine the energies of the HOMO and LUMO levels for organic semiconductors:

- Direct experimental methods: UPS for $IP = -E_{\mathrm{HOMO}}$ and IPES for $EA = -E_{\mathrm{LUMO}}$.
- Using cyclic voltammetry values corrected using equations (6.24) and (6.25).
- Using a combination of UPS for the HOMO and the optical gap calculated using the correlation $E_{\mathrm{LUMO}} = E_{\mathrm{HOMO}} + 1.37 \times \Delta E_o$ for the LUMO.
- Using a combination of cyclic voltammetry and the optical gap: E_{HOMO} calculated from equation (6.24) and the LUMO determined by $E_{\mathrm{LUMO}} = E_{\mathrm{HOMO}} + 1.37 \times \Delta E_o$.

6.3 Molecular orbitals calculated by DFT

In the following, we will give some examples, using hybrid functionals, which are a class of approximations to the exchange-correlation energy functional in DFT that incorporate a portion of exact exchange from HF theory with exchange and correlation from other sources (*ab initio* or empirical). The exact exchange energy functional is expressed in terms of the Kohn–Sham orbitals rather than the density, and therefore it is termed an implicit density functional. One of the most commonly used versions is B3LYP, which stands for Becke, 3-parameter, Lee–Yang–Parr. B3LYP combines the Becke exchange functional and the correlation functional of Lee, Yang and Parr. This functional is

$$E_{xc}^{B3LYP} = E_x^{LDA} + a_0(E_x^{HF} - E_x^{LDA}) + a_x(E_x^{GGA} - E_x^{LDA}) + E_c^{LDA} + a_c(E_c^{GGA} - E_c^{LDA}) \tag{6.26}$$

where $a_0 = 0.20$, $a_x = 0.72$, and $a_c = 0.81$. E_x^{GGA} and E_c^{GGA} are generalized gradient approximations: the Becke-1988 exchange functional and the correlation functional of Lee–Yang–Parr 1988 (LYP88), and E_c^{LDA} is the Vosko–Wilk–Nusair (VWN) local-density approximation to the correlation functional. The three parameters defining B3LYP have been taken without modification from Becke's original fitting of the analogous B3PW91 functional to a set of atomization energies, ionization potentials, proton affinities, and total atomic energies.

Our own calculations were performed with the basis set split valence augmented with polarization function type (d) 6-31G*, using the SPARTAN'10 software package (Spartan, Wave Function Inc. CA).

We start by giving some examples of results of quantum chemical calculations at the DFT-B3LYP level of the frontier orbitals (HOMO and LUMO) of polymer units and small molecules, and show how they can be combined to form the valence band (HOMO band) and the conduction band (LUMO band), respectively, and which, of course, depend on the crystal structure and the magnitude and type of the transfer integrals within the solid. Then, we will show examples of results of band structure calculations based on density functional theory methods. These calculations can give important information on the bandwidths, density of states, Fermi surfaces and other data relevant for the understanding of transport and optical properties.

In figure 6.6, we show the HOMO and LUMO orbitals of a chain of 56 CH units, taken here as a simplified model for a chain of polyacetylene. The calculated values are as follows: $E_{HOMO} = -4.23$ eV, $E_{LUMO} = -2.78$ eV. The HOMO–LUMO gap is 1.45 eV, which compares well with the experimental gap of $E_g \sim 1.2$ eV [10].

In figure 6.7, we give the results for a sequence of six oligomers of p-phenylene vinylene (PV), as units of the conjugated polymer poly(p-phenylene vinylene) (PPV).

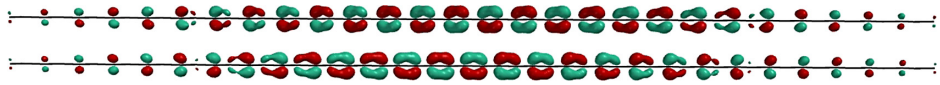

Figure 6.6. The HOMO (top) and LUMO (bottom) orbitals obtained from a DFT/B3YLP calculation for a chain of 56 CH units. $E_{HOMO} = -4.23$ eV, $E_{LUMO} = -2.78$ eV.

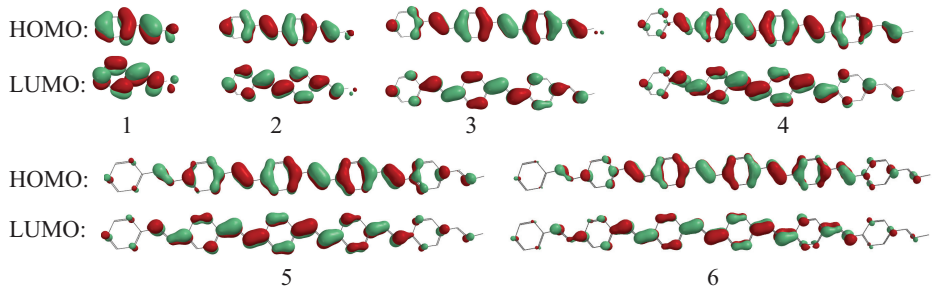

Figure 6.7. Frontier orbitals for 1–6 PV units.

Table 6.1. Molecular orbital frontier levels for PV oligomers.

Oligomer	E_{HOMO}/eV	E_{LUMO}/eV	Gap/eV
PV1	−5.79	−0.67	5.12
PV2	−5.24	−1.51	3.73
PV3	−5.04	−1.83	3.21
PV4	−4.94	−1.99	2.95
PV5	−4.88	−2.08	2.80
PV6	−4.86	−2.14	2.72

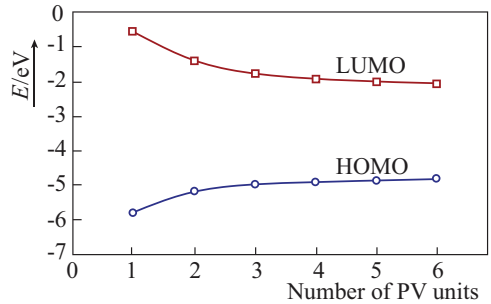

Figure 6.8. Values of frontier orbital energies for 1–6 PV units.

The sequence starts with one unit and goes up to six units. The HOMO and LUMO orbitals are shown.

The respective energies are given in table 6.1, and a plot of the levels as a function of the number of PV units is shown in figure 6.8.

This simple exercise shows that the frontier levels tend to stabilize at constant values, as we increase the number of PV units. For six units, we get a value for the HOMO–LUMO gap of $E_{LUMO} - E_{HOMO} = 2.72$ eV, which is not very far from the experimental value of 2.5 eV. In fact, PPV is a highly stable conjugated polymer and its yellow color is due to an absorption band centered at 400–420 nm.

6.3.1 Small molecules

Anthracene is a wide band gap organic semiconductor due to the π–π interactions between adjacent molecules as in pentacene and other polyacenes. We performed a DFT/B3YLP calculation and found the results for the frontier orbitals shown in figure 6.9.

The crystal structure of anthracene was one of the first crystalline structures of organic compounds to be studied. It was studied by Sir William Bragg himself in the early 1920s [11] and is monoclinic prismatic characterized by the herringbone arrangement with tilted edge-to-face π–π interactions with the following parameters: $a = 8.58$Å, $b = 6.02$ Å, $c = 11.18$ Å, $\beta = 125°$.

The first work on organic light emitting diodes was due to Ching Wan Tang and Steven Van Slyke at Eastman Kodak [12]. It was based on aluminum tris-8-

hydroxyquinoline, best known as Alq_3, and the device structure consisted of indium tin oxide (ITO)/diamine hole transporting later (HTL)/Alq_3/Mg:Ag, meaning a layer of Alq_3 as the electroluminescent and electron transport material sandwiched between two electrodes, a cathode of magnesium–silver alloy with a layer of silver to protect the magnesium, and an anode of transparent ITO deposited on glass. A layer of diamine was used as a HTL. The electrons and holes combine at the diamine/Alq_3 interface.

The Alq_3 molecular structure consists on three hydroxyquinoline ligands bonded to an aluminum atom. Several isomers have been identified, but the so-called *facial* and the *meridional* have been the most studied (see figure 6.10).

The facial (fac) isomer has this name because the three ligands are positioned along one of the faces of the octahedron centered in the Al atom. In the meridional (mer) isomer, the three ligands are positioned along one meridian (a line from one apex of the octahedron to the opposite apex).

The electronic structure of Alq_3 has been studied in many ways and for both 'fac' and 'mer' isomers, in the pristine solid state and when doped with alkali metals, combining experimental and theoretical methods based on x-ray photoelectron emission and absorption spectroscopies, as well as UV photoelectron spectroscopy and DFT quantum chemical calculations including band structure [13–18].

Figure 6.11 shows the molecular structure and the HOMO and LUMO orbitals in the equilibrium geometry of the meridional isomer calculated by quantum chemical DFT at the B3YLP level. As seen in the figure, the HOMO is mainly localized on the phenoxide side of the ligands, while the LUMO is localized on the pyridyl side. Due to the symmetry of the molecule, the frontier orbitals appear in groups of three, meaning, for example, that the LUMO+2 and the LUMO+1 are similar to the

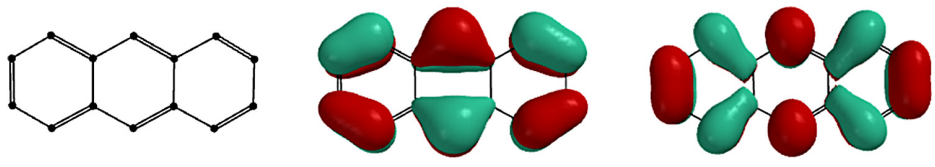

Figure 6.9. HOMO and LUMO orbitals in anthracene. $E_{HOMO} = -5.23$ eV, $E_{LUMO} = -1.63$ eV.

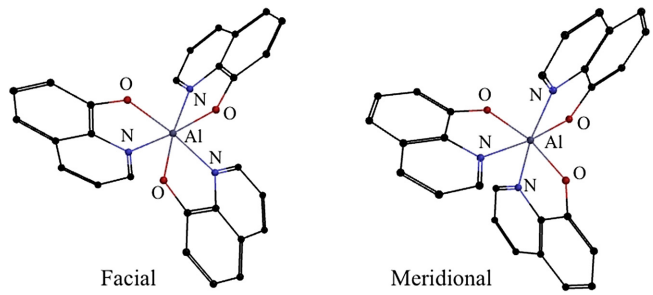

Figure 6.10. Molecular structure of the two best known isomers of Alq_3: the facial and the meridional.

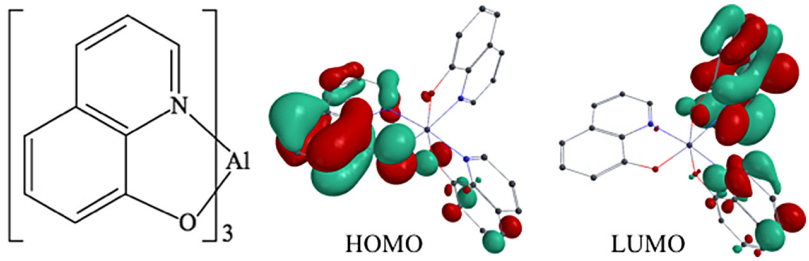

Figure 6.11. Molecular structure of Alq_3, and the HOMO and LUMO orbitals in the equilibrium geometry for the meridional isomer. $E_{HOMO} = -5.01$ eV, $E_{LUMO} = -1.73$ eV, HOMO–LUMO gap =3.28 eV.

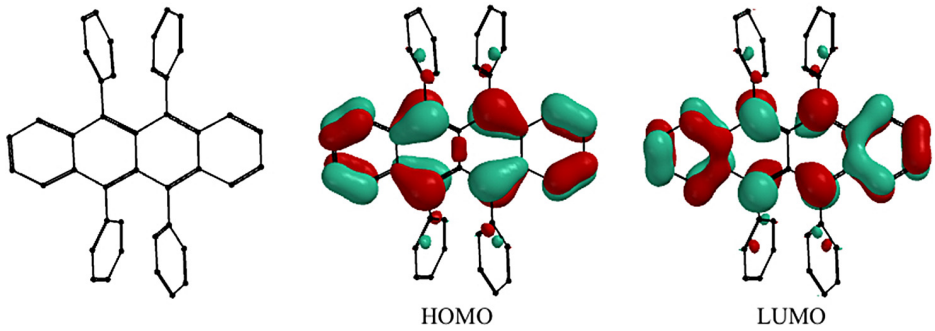

Figure 6.12. Molecular structure of rubrene and HOMO and LUMO orbitals. $E_{HOMO} = -4.61$ eV, $E_{LUMO} = -2.11$ eV.

LUMO, each located on one of the ligands, and the same is found for the HOMO−2, HOMO−1 and HOMO. Naturally, the energy values are similar within each group. For example, the calculated values for the HOMO group are $E_{HOMO} = -5.0$ eV, $E_{HOMO-1} = -5.2$ eV and $E_{HOMO-2} = -5.3$ eV.

Our own calculations on the facial isomer give the following values for the frontier levels: $E_{HOMO} = -5.20$ eV, $E_{LUMO} = -1.68$ eV. Besides the fact that the facial isomer has a slightly higher HOMO–LUMO gap, (3.52 eV vs 3.28 eV), it has a higher dipole moment ($\mu = 7.9$ debye vs $\mu = 4.46$ debye for the 'mer' isomer). These different features are considered important for high performance thin-film OLEDs, however it is argued that both isomers are present in the amorphous films [19].

Rubrene is another small molecule semiconductor considered the standard material for single crystal organic field effect transistors (SC-OFETs). Benchmark carrier mobilities on the range of 20–40 cm^2 V s^{-1} have been achieved in OFETs based on laminated single crystals less than 1 μm thick. A topical review on SC-OFETs is given by Hasegawa *et al* in [20]. In figure 6.12, we show the frontier orbitals as calculated by DFT/B3YLP.

The energies of the frontier levels compare well with those reported by Ma *et al* [21] of $E_{HOMO} = -4.94$eV, $E_{LUMO} = -2.34$ eV, who also report on a DFT detailed study of the electronic structures and conducting properties of rubrene and derivatives, which are characterized by the typical herringbone packing. Carrier

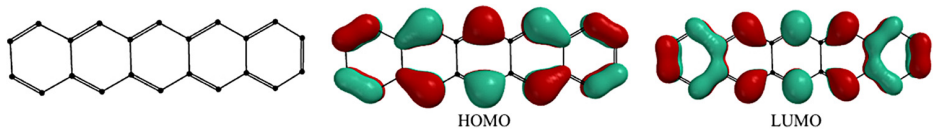

Figure 6.13. Molecular structure and HOMO and LUMO orbitals in pentacene. Energy values: $E_{\mathrm{HOMO}} = -4.60$ eV, $E_{\mathrm{LUMO}} = -2.39$ eV.

mobilities are highly anisotropic (in single crystals). Values in the range of $\mu_h = 1.0$–15.8 $\mathrm{cm^2\ V^{-1}\ s^{-1}}$ are predicted by theory for the hole mobilities, while the found experimental value was $\mu_h = 7.07 \pm 1.77\ \mathrm{cm^2\ V^{-1}\ s^{-1}}$. The theoretical electron mobility was predicted to be in the order of $\mu_e = 0.1$–$3.6\ \mathrm{cm^2\ V^{-1}\ s^{-1}}$.

Last but not least, a few additional words are due about pentacene, the most popular small molecule organic semiconductor for OFETs since the 1980s. The crystal structure and other features of this material have already been discussed. Now we will show the HOMO and LUMO orbitals as obtained from DFT/B3YLP calculations in figure 6.13.

Identical results were obtained by Zhu *et al* [22] using the same density functional (B3LYP/6-31G(d)), namely $E_{\mathrm{HOMO}} = -4.6009$eV, $E_{\mathrm{LUMO}} = -2.3840$ eV and $\Delta E = 2.2169$ eV for the HOMO–LUMO gap.

The values of the frontier levels are close to those of commercial sublimed pentacene $E_{\mathrm{HOMO}} = -4.9$ eV and $E_{\mathrm{LUMO}} = -3.0$ eV, advertised by Ossila, for example.

6.4 Energy bands calculated by DFT

DFT computational methods have been used to calculate band structures of organic semiconductors using various exchange and correlation functionals. Time dependent DFT (TD-DFT) methods are better suited to calculate excited states. The B3LYP hybrid functional is the most popular for calculations on polymer chains although the Kohn–Sham orbital energies generally underestimate the fundamental band gap. Calculations with B3LYP/6-31G* give results which are close to the gaps measured in many conjugated polymers, due to the fact that the errors in orbital energies, geometries, packing and exciton binding energies appear to cancel out. Typical calculations on one-dimensional periodic systems as found in conjugated polymers use, in general, a minimum of 200 **k** points and 100 unit cells. The effective masses, m^*, can be calculated as the inverse curvature of the energy curves of the highest occupied and of the lowest unoccupied crystal orbitals near the extrema, according to the equation

$$\frac{1}{m^*} = \frac{1}{\hbar^2}\frac{d^2\epsilon_k}{dk^2}. \tag{6.27}$$

It has been reported that the B3LYP functional, when compared with other methods, demonstrated better agreement with experimental band gaps of

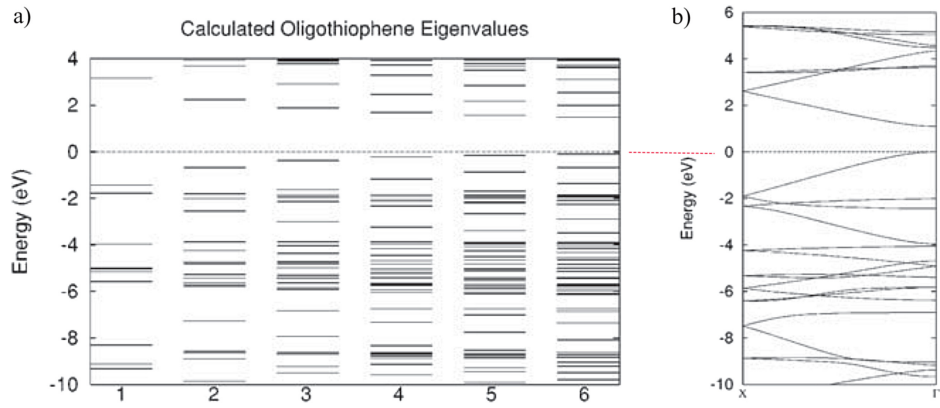

Figure 6.14. (a) Calculated energy levels scaling from oligomers of one to six monomer units. (b) Calculated band structure of polythiophene plotted relative to the valence band maxima. Reprinted figure with permission from [25]. Copyright 2003 by the American Physical Society.

polythiophene (experimental: 2.1 eV, HSE[3]: 1.68 eV, B3LYP: 2.04 eV, BHHLYP[4]: 3.90 eV) [23]. The good agreement between B3LYP and experimental band gaps for semiconducting polymers has also been demonstrated in the theoretical study of periodic organic polymers by Janesko [24].

Hutchison *et al* [25] calculated the energy levels for a series of oligomers with one to six units and the corresponding energy bands using a DFT/LDA method with the Perdew–Wang exchange-correlation functional and a doubled numeric basis set. The results for thiophene oligomers and polythiophene are shown in figure 6.14.

The authors conclude that although DFT methods are used to analyze the scaling of discrete oligomers and give approximate band gaps when extrapolated to infinite polymer chains, the result from that simple extrapolation cannot correctly predict the full band structure of the polymers, namely band crossing, localized bands, and other effects. They also found that the LDA approximation systematically underestimates the band gaps by a factor of ~0.57 when compared with experimental values. This systematic error in the E_g(LDA) has been reported by Brocks and Kelly [26] who recommend that the band gaps calculated by DFT/LDA should be divided by 0.60, as a common procedure. In fact, the LDA calculated gap for polythiophene is 1.10 eV, which divided by 0.6 gives 1.83 eV, much closer to the thin-film experimental value of 2.0 eV.

6.4.1 Band structure of poly(p-phenylene vinylene) (PPV)

The electronic structure of poly(phenylene vinylene) (PPV) has been addressed in section 5.1.2 as an example of how energy bands can be formed in a very intuitive way. Now we will present a more detailed description of the band structure of PPV, as an instructive example.

[3] Heyd–Scuseria–Ernzerhof exchange-correlation functional.
[4] Becke's half-and-half exchange+LYP functional.

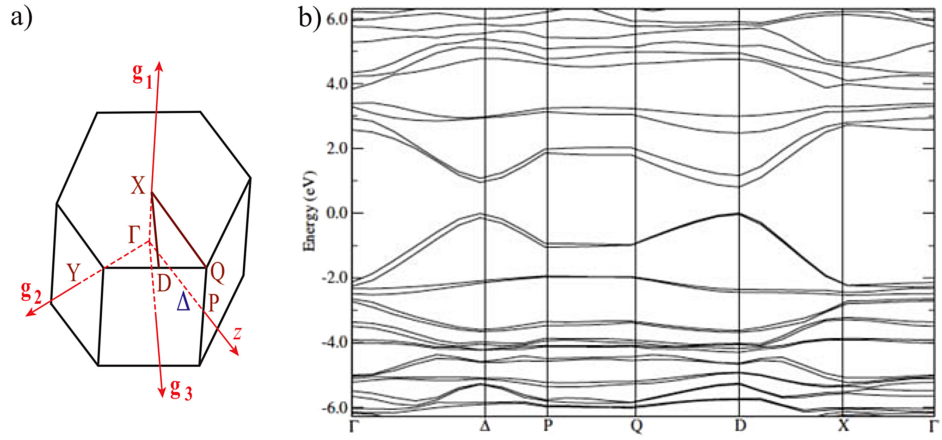

Figure 6.15. (a) Brillouin zone for the PPV monoclinic P_{2_1}/a structure. $\Gamma \rightarrow$ P is the chain direction, where P = (0, −0.355, 0.707) in terms of the reciprocal lattice vectors. Point Δ = (0, −1/4, 1/2) lies at 0.7 of the distance from Γ to P. (b) Band structure for the PPV polymer crystal along the Γ–Δ–P–Q–D–X–Γ path. Energies are in electron volts relative to the top HOMO. From [29]. Reprinted with permission from IOP Publishing.

The crystal structure of PPV is monoclinic P_{2_1}/a with two monomer units per unit cell, in a herringbone arrangement, with the parameters a = 8.07 Å, b = 6.05 Å, c = 6.54 Å, $\alpha = 123°$ [27–29]. Zheng *et al* [29] studied the electronic structure of PPV using a DFT method based on the local density approximation (LDA) with a plane wave basis set and a pseudopotential to describe the electron–ion interactions, which take into account interchain interactions. The band structures were calculated for both an isolated PPV chain and a polymer crystal. The calculation for the single chain gives a HOMO–LUMO band gap of 1.3 eV that is much less than the experimental value of 2.4 eV measured by Voss *et al* [30]. The band structure of the crystalline polymer calculated by Zheng *et al* is displayed in figure 6.15(b) along the paths within the first Brillouin zone defined by the symmetry points indicated in (a).

The main difference between the band structures of the single chain and the polymer crystal is that in the latter the bands occur in pairs due the fact that there are two monomer units per unit cell in the herringbone crystal structure, and the interchain interactions are slightly different for each monomer unit. As expected, the largest bandwidth, with a value of about 2.1 eV, is found along the conjugated chain direction, which corresponds to the $\Gamma \rightarrow$ P path and is of same order of magnitude as for the single chain.

The earlier study of the band structure of PPV by da Costa *et al* [28] is worth to be mentioned because it focus on the interchain coupling and concludes that the ratio between the inter and intrachain transfer integrals, $t_\perp/t_\parallel \approx 0.03$, is quite large. The authors argue that such a value is too large to allow the existence of polarons in a perfect PPV polymer crystal, but that there is evidence that they exist, concluding that their existence is due to defects.

6.4.2 Band structure of pentacene

We cannot finish this chapter without saying a few words about the band structure of pentacene. Several DFT calculations have been done to investigate the band structure of pentacene in the bulk and in the polymorph thin-film as, for example, those in [31–33], to name but a few. Here, we have chosen the Parisse *et al* [33] results as our example. The generalized gradient approximation (GGA) to the exchange-correlation potential was used. Pentacene appears in at least four different phases, depending on the tilting of the molecules relative to the substrate and on the distance between planes along the *c*-axis, features which affect, in particular, the transport properties.

The authors used the results of Campbell *et al* [34] for the crystal structure of the bulk phase, namely that it is triclinic, with two molecules per unit cell of dimensions $a = 7.90$Å, $b = 6.06$ Å, $c = 16.01$ Å; $\alpha = 101.9°$, $\beta = 112.6°$, $\gamma = 85.8°$. For the polymorph thin-film, they used the results of Ruiz *et al* [35]: $a = 7.6$Å, $b = 5.9$ Å, $c = 15.43$ Å; $\alpha = \beta = \gamma = 90°$.

Figure 6.16 reproduces Parisse *et al* band structures for the bulk and for the thin-film polymorphs of pentacene along several symmetry directions.

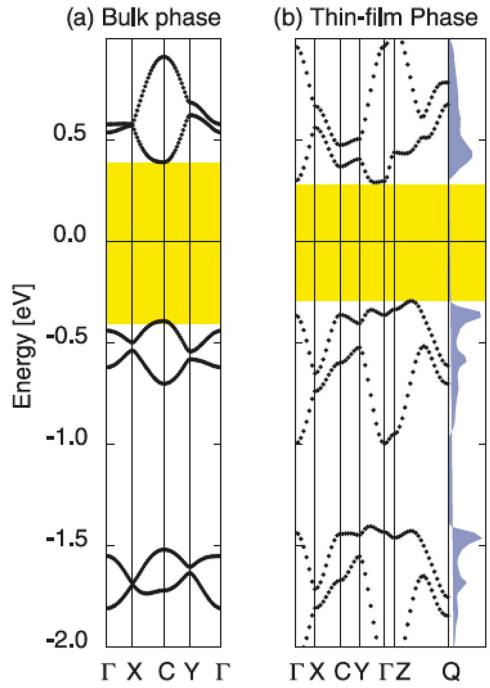

Figure 6.16. DFT/GGA band structure of the bulk phase of pentacene (a) and for the thin-film phase with the density of states (b) along several symmetry directions. Symmetry points: $X = (0.5, 0, 0)$, $Y = (0, 0.5, 0)$, $Z = (0, 0, 0.5)$, $C = (0.5, 0.5, 0)$ and $Q = (0.5, -1, 0.5)$. Energies are referred to the Fermi level. Only the HOMO−1, HOMO and LUMO bands are shown. From [33]. Reprinted with permission from IOP Publishing.

The energy gap is indicated in yellow. From the band structure, it can be seen that the bandwidth is small along the $\Gamma \rightarrow Z$ direction (shown in the thin-film phase) and much larger along the other directions, such as $\Gamma \rightarrow X$ and $\Gamma \rightarrow Y$, in the *ab* plane (see figure 5.12), confirming that the mobility (and conductivity) which depends on the bandwidth is higher in that plane where the π–π intermolecular interactions are predominant. The gap is smaller for the thin-film polymorph, and the valence (HOMO) and conduction (LUMO) bandwidths are reported as ~0.7 and ~0.8 eV, respectively, which are larger than those of the bulk phase. All this is consistent with the higher conductivity observed in thin-films.

Further reading

There are many books and sources on Computational Quantum Chemistry. We particularly recommend the following:

- *Quantum Chemistry. A Concise Introduction for Students of Physics, Chemistry, Biochemistry and Materials Science* [36], an IOP Concise Physics book by Ajit J Thakkar.
- *Quantum Chemistry* by I N Levine [37].
- *Modern Quantum Chemistry: Introduction to Advanced Electronic Structure Theory* by A Szabo and N S Ostlund [38].
- *Introduction to Computational Chemistry* by F Jensen [39].
- *A Chemist's Guide to Density Functional Theory* by W Koch and M C Holthausen [40].

Problems

1. (a) Write the Hamiltonian for the hydrogen atom in atomic units.
   (b) What is the energy of the hydrogen atom in the ground state, in atomic units?
   (c) The STO for the 1s orbital is $\phi_{1s}^{\mathrm{STO}} = Ne^{-\zeta r}$. Calculate the normalization constant N.
2. An *ab initio* HF calculation was made for the water molecule using a 3-21G* basis set. The following linear combination was obtained for the HOMO:

$$\Psi_{\mathrm{HOMO}} = 0.52105 p_y(\mathrm{O}) + 0.63233 \mathrm{p'}_y(\mathrm{O})$$

   with all other coefficients being null. $p_y(\mathrm{O})$ and $p'_y(\mathrm{O})$ are STOs similar to the usual p_y orbitals centered in the O atom. The overlap S matrix relative to these orbitals is

$$\mathbf{S} = \begin{pmatrix} 1 & 0.498767 \\ 0.498767 & 1 \end{pmatrix}.$$

   (a) Calculate the density matrix relative to the HOMO orbital.
   (b) Calculate the electron population associated to the O atom in the HOMO orbital.
   (c) Comment on the result obtained in the last point.

3. Consider the band structure of PPV shown in figure 6.15.
   (a) The largest bandwidth of the conduction band is found along the $\Gamma \rightarrow P$. Why?
   (b) The main optical absorption in PPV starts at about 2.5 eV. What is the value of the optical gap? Why?
   (c) Estimate the value of the optical gap from the band structure in the figure. Compare it with the value predicted from the optical absorption and explain why it is different.
   (d) The bands along $\Gamma \rightarrow X$ and $P \rightarrow Q$ are almost flat. What can you infer from that and why?
4. Compare the band structures of pentacene in the bulk and in thin-films shown in figure 6.16.
   (a) Comment on which phase is expected to exhibit higher conductivity and mobility.
   (b) Comment on the anisotropy of the conductivity and mobility in the thin-film phase.
   (c) From the values of the unit cell dimensions of the two phases of pentacene given in section 6.4.2, calculate their volumes and the densities.

References

[1] Roothaan C C J 1951 *Rev. Mod. Phys.* **23** 69–89
[2] Hohenberg P and Kohn W 1964 *Phys. Rev.* **136** B864–71
[3] Kohn W and Sham L J 1965 *Phys. Rev.* **140** A1133–38
[4] Stowasser R and Hoffmann R 1999 *J. Am. Chem. Soc.* **121** 3414–20
[5] Baerends E J, Gritsenko O V and van Meer R 2013 *Phys. Chem. Chem. Phys.* **15** 16408–25
[6] Zhang G and Musgrave C B 2007 *J. Phys. Chem.* A **111** 1554–61
[7] Bredas J L 2014 *Mater. Horiz.* **1** 17–9
[8] Köhler A and Bässler H 2015 *Electronic Processes in Organic Semiconductors: An Introduction* (New York: Wiley)
[9] Sworakowski J 2018 *Synth. Met.* **235** 125–30
[10] Grant P M and Batra P 1979 *Solid State Commun.* **29** 225–29
[11] Bragg W H 1922 *Proc. Phys. Soc. Lond.* **35** 167
[12] Tang C W and VanSlyke S A 1987 *Appl. Phys. Lett.* **51** 913–15
[13] Curioni A, Andreoni W, Treusch R, Himpsel F J, Haskal E, Seidler P, Heske C, Kakar S, van Buuren T and Terminello L J 1998 *Appl. Phys. Lett.* **72** 1575–77
[14] Curioni A, Boero M and Andreoni W 1998 *Chem. Phys. Lett.* **294** 263–71
[15] Treusch R *et al* 1999 *J. Appl. Phys.* **86** 88–93
[16] Johansson N, Osada T, Stafström S, Salaneck W R, Parente V, dos Santos D A, Crispin X and Brédas J L 1999 *J. Chem. Phys.* **111** 2157–63
[17] Yang Y, Geng H, Yin S, Shuai Z and Peng J 2006 *J. Phys. Chem.* B **110** 3180–84
[18] DeMasi A, Piper L F J, Zhang Y, Reid I, Wang S, Smith K E, Downes J E, Peltekis N, McGuinness C and Matsuura A 2008 *J. Chem. Phys.* **129** 224705
[19] Cölle M, Dinnebier R E and Brütting W 2002 *Chem. Commun.* **23** 2908–09
[20] Hasegawa T and Takeya J 2009 *Sci. Technol. Adv. Mater.* **10** 024314

[21] Ma H, Liu N and Huang J D 2017 *Sci. Rep.* **7** 331
[22] Zhu Z, Wu S and Zhang Y 2008 *Russ. J. Phys. Chem.* A **82** 2293–98
[23] Wong B M and Cordaro J G 2011 *J. Phys. Chem.* C **115** 18333–41
[24] Janesko B G 2011 *J. Chem. Phys.* **134** 184105
[25] Hutchison G R, Zhao Y J, Delley B, Freeman A J, Ratner M A and Marks T J 2003 *Phys. Rev.* B **68** 035204
[26] Brocks G, Kelly P J and Car R 1993 *Synth. Met.* **57** 4243–48
[27] Chen D, Winokur M J, Masse M A and Karasz F E 1990 *Phys. Rev.* B **41** 6759–67
[28] da Costa P G, Dandrea R G and Conwell E M 1993 *Phys. Rev.* B **47** 1800–10
[29] Zheng G, Clark S J, Brand S and Abram R A 2004 *J. Phys.: Condens. Matter* **16** 8609
[30] Voss K F, Foster C M, Smilowitz L, Mihailović D, Askari S, Srdanov G, Ni Z, Shi S, Heeger A J and Wudl F 1991 *Phys. Rev.* B **43** 5109–18
[31] Endres R G, Fong C Y, Yang L H, Witte G and Wöll C 2004 *Comput. Mater. Sci.* **29** 362–70
[32] Troisi A and Orlandi G 2005 *J. Phys. Chem.* B **109** 1849–56
[33] Parisse P, Ottaviano L, Delley B and Picozzi S 2007 *J. Phys.: Condens. Matter* **19** 106209
[34] Campbell R B, Robertson J M and Trotter J 1962 *Acta Crystallogr.* **15** 289–90
[35] Ruiz R, Mayer A C, Malliaras G G, Nickel B, Scoles G, Kazimirov A, Kim H, Headrick R L and Islam Z 2004 *Appl. Phys. Lett.* **85** 4926–28
[36] Thakkar A J 2017 *Quantum Chemistry* 2nd edn (San Rafael, CA: Morgan & Claypool) pp 2053–571
[37] Levine I N 2013 *Quantum Chemistry* 7th edn (New York: Pearson)
[38] Szabo A and Ostlund N S 1996 *Modern Quantum Chemistry: Introduction to Advanced Electronic Structure Theory* (New York: Dover)
[39] Jensen F 2003 *Introduction to Computational Chemistyry* (New York: Wiley)
[40] Koch W and Holthausen M C 2001 *A Chemist's Guide to Density Functional Theory* 2nd edn (New York: Wiley)